International Journal of Applied Pharmaceutics

ISSN- 0975-7058 Vol 18, Issue 1, 2026

Original Article

# QUALITY-BY-DESIGN DEVELOPMENT OF CURCUMIN-LOADED NANOSUSPENSION FOR ENHANCED SOLUBILITY AND SOLIDIFICATION INTO ORAL THIN FILMS

**SHOBHA UBGADE*, VAISHALI KILOR, NIDHI SAPKAL, SHUBHAM GUPTA, ALOK UBGADE, KRISHNAKANT BHELKAR**

*Gurunanak College of Pharmacy, Nagpur-440026, Maharashtra, India
*Corresponding author: Shobha Ubgade; *Email: shobhayadav1402@gmail.com

*Received: 25 Aug 2025, Revised and Accepted: 01 Dec 2025*

**ABSTRACT**

**Objective:** This study aimed to develop and optimize a curcumin (CUR) nanosuspension (NS) to enhance solubility using a Quality-by-Design approach and to solidify the NS into oral thin films (OTFs) as a patient-friendly dosage form.

**Methods:** NS was prepared using high shear homogenization (HSH). Stabilizer concentration and homogenization time were optimized using a factorial design, with particle size, polydispersity index (PDI), and drug loading defined as critical quality attributes. The optimized NS was characterized forsaturation solubility, *in vitro* dissolution, and *in vivo* pharmacokinetics and solidified into OTFs by solvent casting and evaluated.

**Results:** The optimum stabilizer concentration of SLS (0.7%w/v) and homogenization time (190 min) resulted in NS witha particle size (259.8±30 nm),PDI (0.402±0.034), drug loading (61±1.1%),15-fold increase in saturation solubility, and faster dissolution. Pharmacokinetic studyrevealed only modest improvement in oral bioavailability of NS (~1.2-fold) higher relative bioavailability as compared to pure drug. OTFs containing NS demonstrated good mechanical integrity, rapid disintegration (26 sec), preservation of nano-sized particles post-solidification (277.8±46 nm) and enhanced dissolution.

**Conclusion:** A Quality-by-Design-based NS formulation of CUR markedly improved solubility and was successfully solidified into OTFs, offering a stable and convenient oral delivery system.

**Keywords:** Curcumin, Nanosuspension, High shear homogenization, Solubility enhancement, Oral thin films


DOI: https://dx.doi.org/10.22159/ijap.2026v18i1.56641 Journal homepage: https://innovareacademics.in/journals/index.php/ijap

## INTRODUCTION

Curcumin (CUR) is a hydrophobic polyphenolic phytoconstituent derived from *Curcuma longa*, widely recognized for its broad spectrum of pharmacological activities, including anti-inflammatory, antioxidant, anticancer, and neuroprotective effects. Its favorable safety profile and therapeutic versatility have generated considerable global interest. However, the clinical translation of CUR remains challenging due to its poor biopharmaceutical properties. Classified as a Biopharmaceutics Classification System (BCS) Class IV drug, CUR exhibits extremely low aqueous solubility and minimal gastrointestinal permeability, leading to poor and variable oral bioavailability [1, 2].

To address these limitations, various solubility enhancement strategies have been explored, including cyclodextrin inclusion complexes [3], solid dispersions [4], and solid self-microemulsifying drug delivery systems (S-SMEDDS) [5]. Particle size reduction methods-such as nanoparticles [6], nanosuspensions (NS) [7], manipulation of solid-state crystallinity, and prodrug synthesis [8] have also been investigated. While these approaches can improve solubility, many require complex manufacturing processes or multiple excipients, which may hinder scalability and cost-effectiveness in industrial production.

Particle size reduction is among the most effective and widely adopted methods for enhancing the dissolution and solubility of poorly water-soluble drugs, owing to the increased surface area [9]. Nanosizing, typically producing particles in the 10–1000 nm range, can enhance both solubility and bioavailability. Nanosuspensions are colloidal dispersions of pure drug particles, stabilized by surfactants or polymers, with mean particle sizes below 1 µm [10]. This carrier-free delivery system can markedly improve dissolution velocity and apparent solubility, making it a promising platform for drugs like CUR.

Despite these advantages, NS are thermodynamically unstable due to their high surface energy, which promotes agglomeration and Ostwald ripening [11]. Stability can be improved by careful selection of stabilizer type and concentration, and by employing solidification techniques to convert the liquid NS into a stable solid dosage form. However, only few studies have reported the direct solidification of CUR NS into final dosage forms suitable for patient use.

In this study, a stable CUR NS was developed and optimized for enhanced solubility, followed by its conversion into oral thin films (OTFs) as a convenient solidified dosage form. High shear homogenization (HSH) was employed as a simple and scalable particle size reduction technique. Preliminary screening identified key formulation and process parameters, which were subsequently optimized using a two-factor, three-level factorial design. The optimized liquid NS was extensively characterized for physicochemical attributes, *in vitro* dissolution, and *in vivo* pharmacokinetics, and then solidified into OTFs as a model approach for improving stability and patient compliance.

## MATERIALS AND METHODS

### Materials

Curcumin (CUR), hydroxypropyl methylcellulose (HPMC E15), polyvinylpyrrolidone K30 (PVP-K30), and polyvinyl alcohol (PVA) were kindly provided by Zim Laboratories Ltd., Kalmeshwar, Nagpur, India. D-α-Tocopheryl polyethylene glycol 1000 succinate (Vitamin E TPGS) was received from Matrix Fine Sciences Pvt. Ltd., Aurangabad, India. Poloxamer 188, poloxamer 407, sodium lauryl sulfate (SLS), and polyethylene glycol 400 (PEG 400) were obtained from Himedia Laboratories Pvt. Ltd., Mumbai, India. Tween 80 was purchased from Merck India Ltd. All other reagents and chemicals were of analytical grade.

### Preliminary screening of parameters for nanosuspension (NS) preparation

Initial screening of formulation and process parameters-type and concentration of stabilizer, homogenization speed, and homogenization time-was conducted using a one-variable-at-a-time (OVAT) approach. Stabilizers from various classes were evaluated:

nonionic surfactants (poloxamer 188, poloxamer 407, Tween 80), polymeric stabilizers (PVP-K30, HPMC E15, PVA), anionic surfactant (SLS), and amphiphilic stabilizer (Vitamin E TPGS). Stabilizer selection was based on CUR solubility in the stabilizer solution (shake-flask method) and wettability improvement (contact angle measurement) [12]. Drug-to-stabilizer ratios of 1:1, 1:2, and 1:4 were tested. NS formulations were prepared at a fixed homogenization speed (10,000 rpm) with homogenization times ranging from 90 to 270 min.

**Preparation of CUR-loaded NS**

CUR-NS was prepared using a top-down approach via high shear homogenization (Kinematica Polytron PT 3100 D, Switzerland). CUR powder was dispersed in an aqueous stabilizer solution containing fixed amount of poloxamer 188 (500 mg) and SLS, followed by homogenization to produce NS batches. Formulations were stored in amber glass containers at 4 °C until further evaluation.

**Design of experiments (DoE) optimization**

A two-factor, three-level factorial design [13] was employed, yielding a total of ten experimental runs including one replicate. The independent variables were SLS concentration (drug-to-stabilizer ratio) and homogenization time; the dependent variables were particle size, polydispersity index (PDI), and drug loading. Levels of each variable and the experimental design matrix are shown in tables 1 and 2.

**Table 1: The level of variables in $3^2$ factorial design**

| Factors | Low | Medium | High |
|---|---|---|---|
| Conc. of SLS (Drug: Stabilizer ratio) | 1:0.5 | 1:1 | 1:2 |
| Homogenization time (min) | 90 | 180 | 270 |

**Table 2: Design matrix for preparation and optimization of CUR NS**

| Run | Formulation code | Factor 1 conc. of SLS (Drug: stabilizer ratio) | Factor 2 homogenization time (min) |
|---|---|---|---|
| 1 | C1 | 1:0.5 | 90 |
| 2 | C2 | 1:0.5 | 270 |
| 3 | C3 | 1:1 | 90 |
| 4 | C4 | 1:2 | 180 |
| 5 | C5 | 1:2 | 270 |
| 6 | C6 | 1:1 | 180 |
| 7 | C7 | 1:2 | 90 |
| 8 | C8 | 1:1 | 180 |
| 9 | C9 | 1:1 | 270 |
| 10 | C10 | 1:0.5 | 180 |

**Data analysis and model validation**

Experimental data were fitted to polynomial equations, including interaction terms, using multiple linear regression analysis (Design Expert® v7, Stat-Ease Inc., Minneapolis, USA). Analysis of variance (ANOVA) assessed model significance. Response surface methodology was used to generate 2D contour and 3D plots. The optimal formulation was determined via numerical optimization, targeting a desirability value close to 1. Model validation was performed by preparing and evaluating three checkpoint formulations.

**Preparation of oral thin films (OTFs) of CUR-loaded NS**

OTFs were prepared by solvent casting. HPMC E15 (1 g) and PEG 400 (0.15 g) were incorporated into CUR-NS containing the equivalent of 100 mg CUR, and the mixture was stirred magnetically for 30 min. The resulting solution was cast onto a glass plate and dried in a hot air oven at 50 °C for 2 h. Films were removed with a sharp blade, cut into 2 × 1 cm strips, wrapped in aluminium foil, and stored in a desiccator. These were labelled CNSOTF. Control films prepared with pure CUR powder were labelled COTF [14].

**Characterization of nanosuspension**

**Fourier transform infrared spectroscopy (FTIR)**

Infrared spectrums of pure drug, excipients and drug-excipient physical mixture were recorded using FTIR (Shimadzu FTIR-8101) according to the KBr disk method. The chemical integrity of the drug was determined by comparing the infrared (IR) spectra.

**Differential scanning calorimetry (DSC)**

DSC analysis (DSC 1, Mettler-Toledo, Switzerland) was conducted on CUR, physical mixtures, and the optimized NS. Samples (2–4 mg) were sealed in aluminum pans and heated from 30 °C to 300 °C at 10 °C/min under nitrogen flow (40 ml/min) [15].

**X-ray powder diffraction (XRPD)**

XRPD patterns of CUR and dried NS were obtained using an X-ray diffractometer (Rigaku SmartLab, Japan) with Cu Kα radiation (λ = 1.542 Å) over a 2θ range of 5°–50° [16].

**Particle size and zeta potential**

Measured via photon correlation spectroscopy (Zetasizer Nano ZS 90, Malvern Instruments Ltd., UK) at 25 °C and 90° scattering angle. Samples were diluted (1:10) with bidistilled water. Zeta potential was determined at 25 V/m field strength [17]. Results are expressed as mean±SD (n = 3).

**Drug loading**

One milliliter of NS was diluted to 10 ml with methanol, filtered, and analyzed by UV spectrophotometry (λmax = 425 nm) using methanol as blank [18].

**Saturation solubility**

CUR coarse powder (10 mg) and NS (equivalent to 10 mg CUR) were separately suspended in 10 ml distilled water and shaken at 37 °C for 48 h. Supernatants were filtered and analyzed by UV spectrophotometry [14].

***In vitro* dissolution**

Dissolution testing (USP II) was performed for CUR coarse powder and equivalent NS in 900 ml of 0.5% w/v SLS solution at 50 rpm and 37±0.5 °C for 2 h. Samples (5 ml) were withdrawn at predetermined intervals, replaced with fresh medium, and analyzed spectrophotometrically at 425 nm.

**Stability studies (Liquid NS)**

Optimized NS was stored in light-resistant containers at 2–8 °C for 3 mo. Particle size and drug loading were measured monthly [19].

***In vivo* pharmacokinetic study**

Animal experiments were approved by the Institutional Animal Ethics Committee (Approval No. PH/IAEC/VNS/2K21/09) and conducted according to CPCSEA guidelines. Healthy Wistar rats (150–200 g) were fasted overnight before dosing. Group I (n=6) received pure CUR suspension (75 mg/kg), and Group II (n=6) received CUR-NS (75 mg/kg)) orally. Blood samples were collected at 0, 0.5, 1, 1.5, 2, 3, 6, 10, 12, 24, and 48 h post-dose via retro-orbital

plexus into heparinized tubes, centrifuged (10,000 rpm, 10 min, 2–4 °C), and plasma separated. Plasma proteins were precipitated with acetonitrile (300 µl** per 200 µl** plasma), centrifuged, and supernatants analyzed by HPLC (C18 column, methanol: water mobile phase, 1 ml/min, 20 µl** injection, detection at 420 nm). Pharmacokinetic parameters-t½, Cmax, Tmax, $AUC_0$–t, $AUC_0$–∞, and relative bioavailability (Frel)-were calculated using PKSolver 2.0. Statistical analysis was done using paired t-test to evaluate any significant difference.

**Characterization of NS-loaded OTFs**

**Thickness**

The thickness of the films was measured using the digital micrometre with an accuracy of 0.001 mm. Thickness was measured for 10 different films and average thickness was determined [14, 20].

**Tensile strength**

Tensile strength of film was determined by tensile strength instrument (Saurashtra SystopackPvt. Ltd., Mumbai). To determine the tensile strength, polymeric films were sandwiched separated by corked linear iron plates. One end of the film was kept fixed with the help of an iron screw and the other end was connected to a freely movable iron screw over a pulley. Tensile strength is the maximum stress applied to a point at which the film specimen breaks. It was calculated by the applied load at rupture divided by the cross-sectional area of the film.

**Folding endurance**

Determined by repeatedly folding the film at the same point until breakage. The number of times the film is folded without breaking is computed as the folding endurance value. The folding endurance studies were performed for six strips for each batch i. e. CNSOTF and COTF [14, 21].

**Moisture absorption**

Films were placed at 75±2% RH (NaCl-saturated desiccator) until constant weight; % moisture uptake was calculated.

**Disintegration time**

*The disintegration* test was performed using simulated salivary fluid (pH 6.8) as the medium. One film was held in a beaker containing 100 ml of medium maintained at 37 °C±2 °C, and the time required to disintegrate the film was noted. The average disintegration time of six films was noted for both the batches [14, 21].

**Drug content**

Six random films were sonicated with methanol (10 ml) for 2 h, filtered, diluted, and analyzed by UV spectrophotometry (425 nm).

***In vitro* dissolution**

It was conducted for CNSOTF and COTF (equivalent to 10 mg CUR) in 900 ml simulated salivary fluid (pH 6.8) at 75 rpm and 37±0.5 °C. Samples (5 ml) were withdrawn at intervals and analyzed spectrophotometrically at λmax 425 nm. The determinations were carried out in triplicate, and results were expressed as mean±SD [14, 22].

**Redispersibility**

Prepared
NS-loaded films were immersed in a beaker containing distilled water and sonicated to redisperse the solidified NS. The sample was filtered and assessed for mean particle size using method reported earlier for particle size analysis. The determinations were carried out in triplicate and results were expressed as mean±SD [23]

**Stability studies (Solid OTFs)**

CNSOTF samples were stored under accelerated conditions (40±2 °C/75±5% RH) for 3 mo, with evaluations for disintegration time, redispersibility, drug content, and dissolution profile at 1, 2, and 3 mo. The determinations were carried out in triplicate and results were expressed as mean±SD.

**RESULTS AND DISCUSSION**

**Preliminary screening of parameters for NS preparation**

Saturation solubility and contact angle measurements were used to identify a stabilizer with maximum wetting ability and minimal solubilization, thereby reducing the risk of Ostwald ripening.

CUR exhibited the highest solubility in PVP K30, while the lowest was observed in Poloxamer 188, followed by SLS. Since high solubility in stabilizer solution can promote Ostwald ripening and increase particle size during storage, Poloxamer 188 and SLS were preferred. Contact angle measurements confirmed that both exhibited the lowest angles with CUR, indicating optimal wetting properties for size reduction (fig. 1).

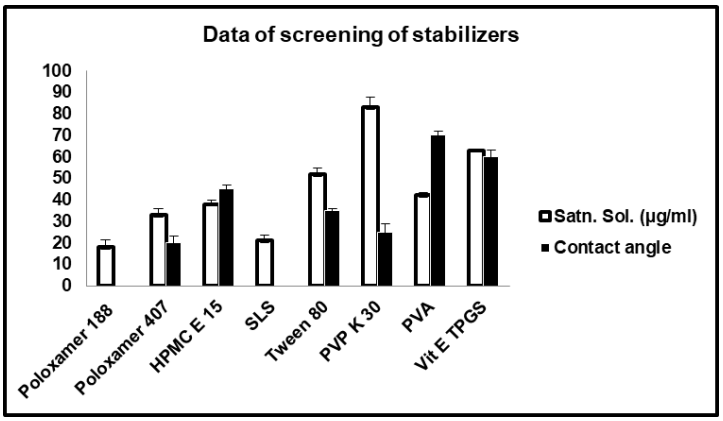


**Fig. 1: Saturation solubility and contact angle measurement data of various screened stabilizers for curcumin nanosuspension*, (n=3)**
***Mean±SD**

Homogenization was performed at a constant speed of 10,000 rpm with varying times (90, 180, and 270 min).

**Design of experiment–based optimization of NS**

CUR NS optimization was performed using a 2-factor, 3-level factorial design, as only two parameters-amount of surfactant and homogenization time-were selected for optimization. The design comprised 10 experimental runs, including one center point. Factorial designs enable the evaluation of all factor levels in combination, making them widely used in response surface optimization.

**Data analysis, statistical optimization, and model validation**

The experimental runs and observed responses ($Y_1$: particle size, $Y_2$: PDI, $Y_3$: drug loading) are summarized in table 3. The

selected quadratic model provided a good fit for all responses, with ranges of 310–717.5 nm for particle size, 0.433–0.902 for PDI, and 38–66% for drug loading. The design summary is presented in table 4.

**Table 3: $3^2$Factorial design: compositions of variables and recorded responses**

| Run no. | Formulation code | Independent variables | | Responses | | |
|---|---|---|---|---|---|---|
| | | Conc. of SLS (Drug: stabilizer ratio) | Homo. time | Particle size (nm) $Y_1$ | PDI $Y_2$ | % Drug loading $Y_3$ |
| 1 | C1 | 0.5 | 90 | 717.5 | 0.902 | 38 |
| 2 | C2 | 0.5 | 270 | 635 | 0.587 | 44 |
| 3 | C3 | 1 | 90 | 470.6 | 0.668 | 45 |
| 4 | C4 | 2 | 180 | 314.2 | 0.458 | 62 |
| 5 | C5 | 2 | 270 | 310 | 0.433 | 66 |
| 6 | C6 | 1 | 180 | 418 | 0.521 | 52 |
| 7 | C7 | 2 | 90 | 380 | 0.494 | 59 |
| 8 | C8 | 1 | 180 | 416 | 0.516 | 52 |
| 9 | C9 | 1 | 270 | 398 | 0.510 | 57 |
| 10 | C10 | 0.5 | 180 | 670 | 0.816 | 42 |

**Table 4: Design summary of responses**

| Response | Name | Units | Obs | Analysis | Minimum | Maximum | Mean | Std. Dev. | Ratio | Trans | Model |
|---|---|---|---|---|---|---|---|---|---|---|---|
| $Y_1$ | Particle size | nm | 10 | Polynomial | 310 | 717.5 | 472.9 | 140.4 | 2.315 | None | Quadratic |
| $Y_2$ | PDI | | 10 | Polynomial | 0.433 | 0.902 | 0.591 | 0.149 | 2.083 | None | Quadratic |
| $Y_3$ | Drug loading | %t | 10 | Polynomial | 38 | 66 | 51.70 | 8.821 | 1.737 | None | Quadratic |

**Particle size**

Particle sizes across the 10 experimental runs ranged from 310 to 717.5 nm. The quadratic model was statistically significant (model $F$ = 735.18) with a non-significant lack of fit, confirming model adequacy. ANOVA revealed that the linear terms ($A$: surfactant concentration, $B$: homogenization time) and the quadratic terms ($A^2$, $B^2$) significantly influenced particle size ($p$<0.05) as shown in table 5.

**Table 5: ANOVA for response surface quadratic model of particle size**

| Response 1 Particle size, ANOVA for selected quadratic model, Analysis of variance table [Partial sum of squares – Type III] | | | | | | |
|---|---|---|---|---|---|---|
| **Source** | **Sum of squares** | **df** | **Mean square** | **F value** | **p-value Prob>F** | |
| Model | 1970E+005 | 5 | 39391.82 | 735.18 | <0.0001 | Significant |
| A-Conc SLS | 1.728E+005 | 1 | 1.728E+005 | 3225.44 | <0.0001 | not significant |
| B-Time | 8158.94 | 1 | 8158.94 | 152.27 | 0.0002 | |
| AB | 32.94 | 1 | 32.94 | 0.61 | 0.4768 | |
| $A^2$ | 39192.13 | 1 | 39192.13 | 731.46 | <0.0001 | |
| $B^2$ | 756.00 | 1 | 756.00 | 14.11 | 0.0198 | |
| Residual | 214.32 | 4 | 53.58 | | | |
| Lack of Fit | 212.32 | 3 | 70.77 | 35.39 | 0.1228 | |
| Pure Error | 2.00 | 1 | 2.00 | | | |

The regression equation in coded terms was: Particle+343.53−169.72A−37.20B+2.82AB+148.92$A^2$+18.00$B^2$

Negative coefficients for $A$ and $B$ indicate an antagonistic effect, meaning that increasing surfactant concentration or homogenization time reduced particle size. The corresponding 3D response surface plot is shown in fig. 2a.

**Polydispersity index (PDI)**

PDI values varied between 0.433 and 0.902. The quadratic model was significant ($F$ = 17.37) with a significant lack of fit. ANOVA indicated that $A$, $B$, and $A^2$ had a statistically significant impact ($p$<0.05)as shown in table 6.

The regression equation was: PDI=+0.48−0.15A−0.082B+0.060AB+0.12$A^2$+0.011$B^2$

The negative coefficients for $A$ and $B$ demonstrate that higher surfactant concentration and longer homogenization times reduced PDI, indicating improved size uniformity (fig. 2b).

**Drug loading**

Drug loading ranged from 38% to 66%. The quadratic model was significant ($F$ = 53.84), with both $A$ and $B$ having a significant positive effect ($p$<0.05) as shown in table 7.

The regression equation was: Drug loading =+55.67+10.50A+4.16B – 0.054AB – 3.46$A^2$ – 0.57$B^2$

Positive coefficients for $A$ and $B$ indicate that increasing surfactant concentration andhomogenization time enhanced drug loading (fig. 2c).

**Numerical optimization and model validation**

Numerical optimization was conducted using the Design-Expert® software to minimize particle size and PDI while maximizing drug loading. The optimal formulation was predicted at a surfactant concentration of 0.7% w/v and a homogenization time of 190 min.

Under these conditions, the predicted responses were: Particle size: 329.9 nm, PDI: 0.47 and Drug loading: 60.6%

To validate the model, the optimized formulation was prepared in triplicate and evaluated. The observed results (particle size: 259.8±30 nm; PDI: 0.402±0.034; drug loading: 61.0±1.1%)were in close agreement with the predicted values, confirming the reliability of the optimization model.

**Characterization of optimized nanosuspension**

**Fourier transform infrared (FTIR) spectroscopy**

The FTIR spectrum of pure CUR exhibited characteristic peaks at 3505 $cm^{-1}$ (O–H stretching), 1627 $cm^{-1}$ (C=O stretching), 1508 $cm^{-1}$

(aromatic C=C stretching), and 1430 $cm^{-1}$ (phenolic and enolic C–O stretching), consistent with literature reports (fig. 3). The physical mixture showed no significant shifts in peak positions, suggesting no chemical interaction between CUR and the stabilizers.

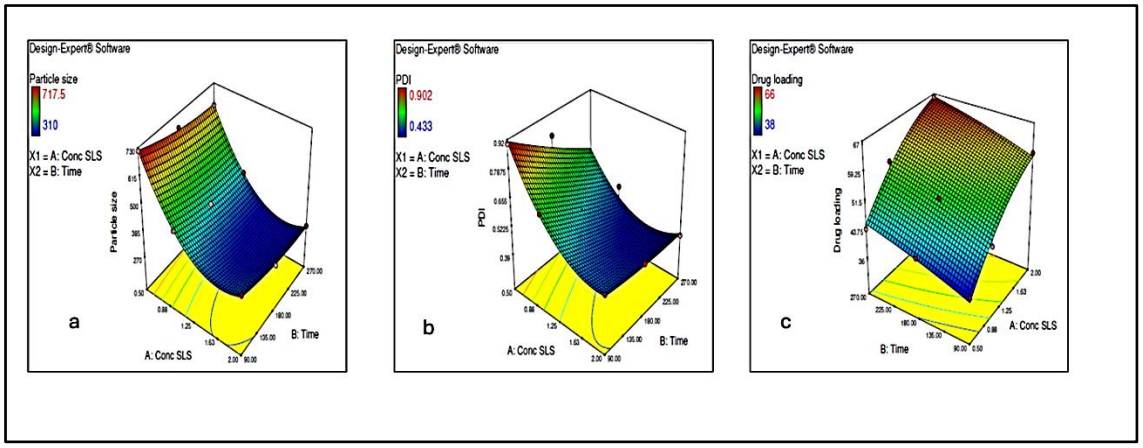


**Fig. 2: Response surface plots illustrating the effect of concentration of SLS and homogenization time on a) Particle size b) PDI c) Drug loading**

**Table 6: ANOVA for response surface quadratic model of PDI**

| Response 2 PDI, ANOVA for selected quadratic model, Analysis of variance table [Partial sum of squares – type III] | | | | | | |
|---|---|---|---|---|---|---|
| **Source** | **Sum of squares** | **df** | **Mean square** | **F value** | **p-value Prob>F** | |
| Model | 0.21 | 5 | 0.043 | 17.37 | 0.0081 | Significant |
| A-Conc SLS | 0.14 | 1 | 0.14 | 57.63 | 0.0016 | significant |
| B-Time | 0.040 | 1 | 0.040 | 16.34 | 0.0156 | |
| AB | 0.015 | 1 | 0.015 | 6.02 | 0.0701 | |
| $A^2$ | 0.027 | 1 | 0.027 | 11.15 | 0.0289 | |
| $B^2$ | 3.010E-004 | 1 | 3.010E-004 | 0.12 | 0.7435 | |
| Residual | 9.792E-003 | 4 | 2.448E-003 | | | |
| Lack of Fit | 9.779E-003 | 3 | 3.260E-003 | 260.78 | 0.0455 | |
| Pure Error | 1.250E-005 | 1 | 1.250E-005 | | | |

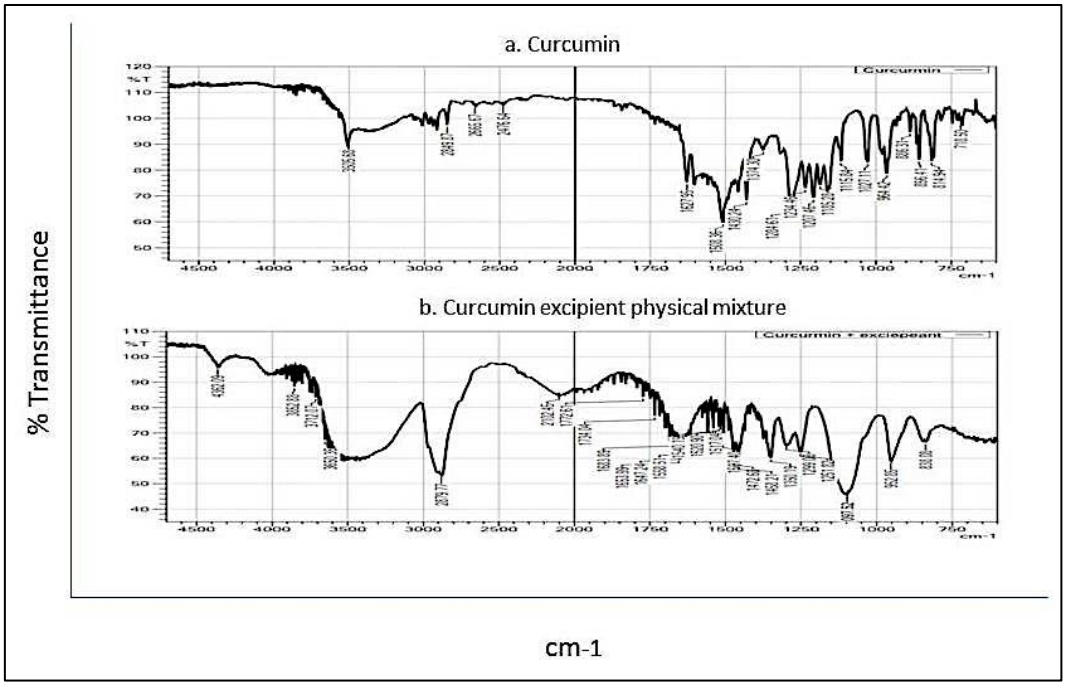


**Fig. 3: FTIR spectra of a) Pure Curcumin, b) Curcumin and excipients physical mixture**

**Differential scanning calorimetry (DSC)**

Pure CUR displayed a sharp melting endotherm at 180 °C, confirming its crystalline nature. The physical mixture exhibited an additional endothermic peak at 57 °C corresponding to the melting of the stabilizers. In the optimized nanosuspension, the CUR melting peak was broadened and shifted to 118 °C, reflecting nanoscale melting point depression and possible stabilizer interactions (fig. 4).

**Table 7: ANOVA for response surface quadratic model of drug loading**

| Response 3 drug loading, ANOVA for selected quadratic model, Analysis of variance table [Partial sum of squares – Type III] | | | | | | |
|---|---|---|---|---|---|---|
| **Source** | **Sum of squares** | **df** | **Mean square** | **F value** | **p-value prob>F** | |
| Model | 766.71 | 5 | 153.34 | 53.84 | 0.0009 | significant |
| A-Conc. SLS | 661.50 | 1 | 661.50 | 232.25 | 0.0001 | |
| B-Time | 102.05 | 1 | 102.05 | 35.83 | 0.0039 | |
| AB | 0.012 | 1 | 0.012 | 4.180E-003 | 0.9516 | |
| $A^2$ | 21.10 | 1 | 21.10 | 7.41 | 0.0529 | |
| $B^2$ | 0.76 | 1 | 0.76 | 0.27 | 0.6323 | |
| Residual | 11.39 | 4 | 2.85 | | | |
| Lack of Fit | 11.39 | 3 | 3.80 | | | |
| Pure Error | 0.000 | 1 | 0.000 | | | |

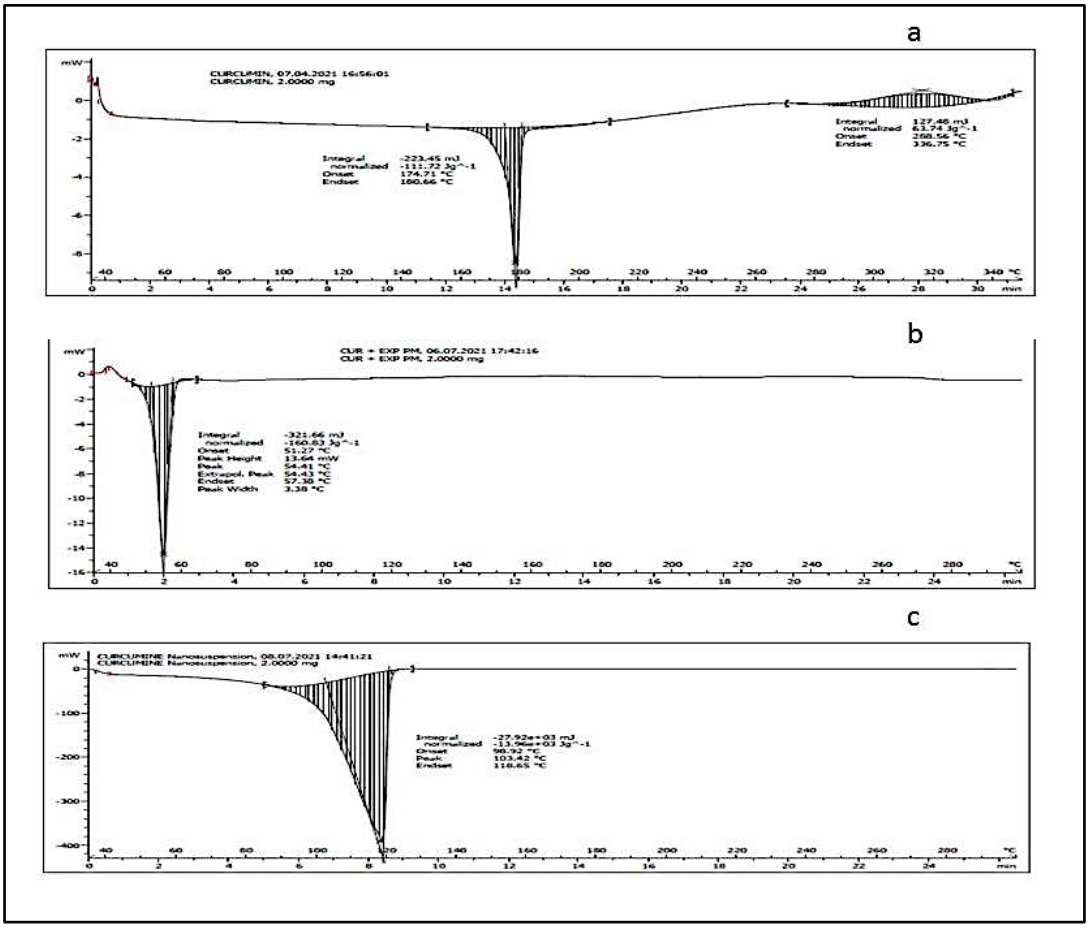


**Fig. 4: DSC thermograms of a) Pure curcumin, b) Curcumin and excipients physical mixture, c) Curcumin nanosuspension**

**X-Ray powder diffraction (XRPD)**

XRPD analysis revealed distinct diffraction peaks for pure CUR at 2θ values of 17° and other characteristic angles, confirming its crystalline structure (fig. 5). The optimized nanosuspension retained the major CUR peaks, suggesting partial crystallinity after size reduction.

**Particle size distribution and zeta potential**

Dynamic light scattering analysis showed a mean particle size of 259.8±30 nm (fig. 7a) and a narrow PDI of 0.402±0.034, indicating uniform distribution. The zeta potential was –22.0±4.5 mV, adequate for combined electrostatic and steric stabilization. The negative zeta potential is likely due to the presence of SLS and surface charge imparted thereof.

**Saturation solubility**

The nanosuspension exhibited a 15-fold increase in saturation solubility (627.4±2.46 µg/ml) compared to pure CUR (40.23±1.69 µg/ml), attributable to the reduced particle size and increased surface area.

***In vitro* dissolution**

The nanosuspension demonstrated significantly faster dissolution, releasing ~75% of CUR within 30 min compared to ~8% from the pure drug (fig. 8 a). This enhancement can be ascribed to the increased surface area and wetting efficiency imparted by the stabilizers.

**Stability studies**

The optimized CUR nanosuspension was stored at 4 °C and 25 °C for three months to assess physical stability. No visible sedimentation or aggregation was observed at either temperature. Particle size, PDI, and zeta potential remained within ±5% of initial values, confirming good stability. The retention of nanoscale size and low PDI suggests that the selected stabilizer system effectively prevented Ostwald ripening and agglomeration.

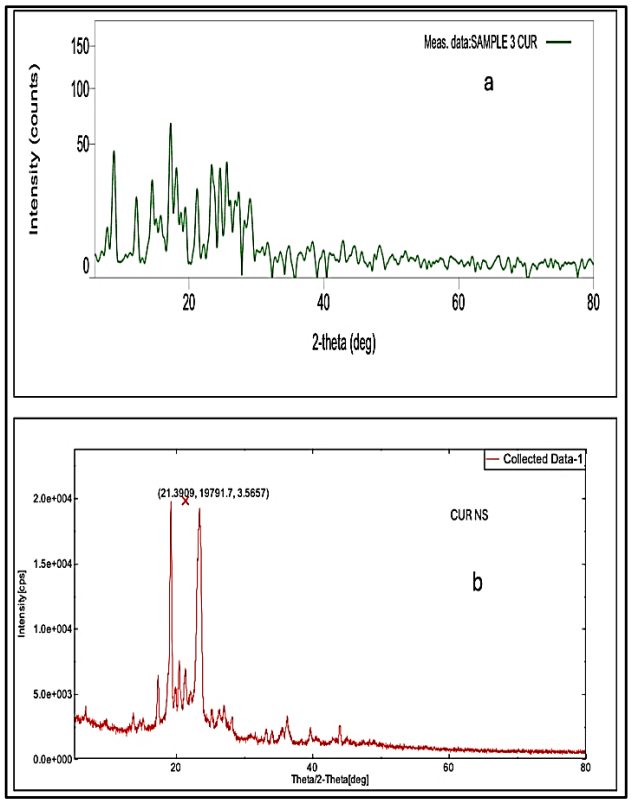


**Fig. 5: Diffractogram of a) CUR and b) CUR NS**

### *In vivo* pharmacokinetic study

Pharmacokinetic evaluation was conducted in rats following a single oral dose of CUR nanosuspension and pure CUR suspension. Plasma CUR concentrations were quantified by validated HPLC. The nanosuspension group exhibited a slightly higher *C*max(3995 ng/ml) compared to the pure drug suspension (3233 ng/ml). The area under the plasma concentration–time curve (AUC) was also modestly greater for the nanosuspension (27606 ng/ml. hr) compared to the pure drug (25089 ng/ml. hr). The statistical analysis of PK data revealed no significant difference ($p>0.05$) amongst tested samples. These results indicate that while the nanosuspension substantially improved solubility and dissolution, the oral bioavailability enhancement *in vivo* was moderate, likely due to CUR's inherent permeability limitations (fig. 6).

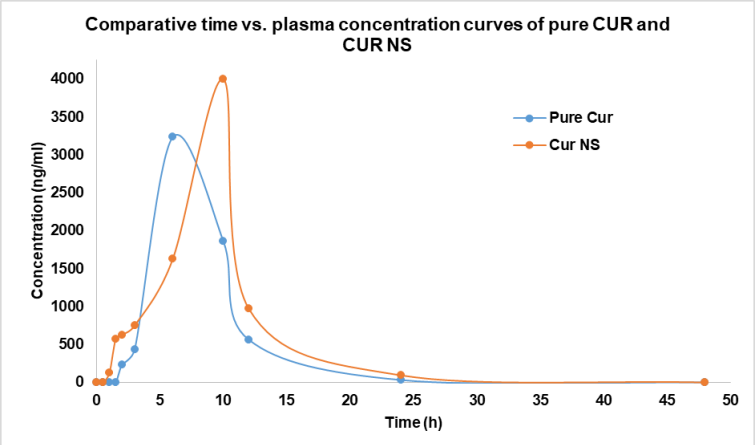


**Fig. 6: Plasma concentration profiles of pure CUR and CUR NS**

### Preparation of oral thin films (OTFs)

OTFs containing either CUR nanosuspension (CNSOTF) or unprocessed CUR (COTF) were fabricated via the solvent casting method using HPMC E15 as the film-forming polymer and PEG 400 as the plasticizer. The optimized CUR nanosuspension was directly incorporated into the polymeric dispersion to ensure uniform nanoscale drug distribution within the film matrix. Films were cast on glass plates and dried at ambient temperature to yield non-sticky, flexible films with uniform thickness.

### Characterization of NS-loaded OTFs

Both COTF and CNSOTF were smooth, translucent, and exhibited good handling properties. Mechanical evaluation indicated that CNSOTF maintained adequate tensile strength and folding endurance suitable for patient use (table 8).

**Table 8: Characterization of COTF and CNSOTF**

| S. No. | Parameters | Formulation code | |
|---|---|---|---|
| | | COTF | CNSOTF |
| 1 | Appearance | Translucent film with smooth surface | Translucent film with smooth surface |
| 2 | Thickness* (mm) | 0.163±2 | 0.145±1 |
| 3 | Tensile strength* (N/mm²) | 37.21±0.8 kg/cm² | 22.06±1.3 kg/cm² |
| 4 | Folding endurance* | 17±2 | 19±3 |
| 5 | (%) Moisture Absorption* | 9.87 ±0.58 | 8.25±1.06 |
| 6 | Disintegration Time* (sec) | 29.12±1.66 | 26.43±0.40 |
| 7 | Drug content* (%) | 95.72±2.6 | 98.65± 1.5 |

(n=3) *Mean±SD

**Redispersibility study**

Redispersion studies confirmed that nanoscale particle size was retained after film formation. The mean particle size of redispersed CNSOTF was 277.8±46 nm, closely matching the original nanosuspension size (259.8±30 nm) (fig. 7a), indicating no significant aggregation during processing (fig. 7b).

***In vitro* drug release**

Dissolution testing in simulated saliva (pH 6.8) revealed rapid and complete release of CUR from CNSOTF, with>95% drug release within minutes (fig. 8b). In contrast, COTF exhibited<20% release over the same period, highlighting the dramatic dissolution enhancement conferred by nanosizing.

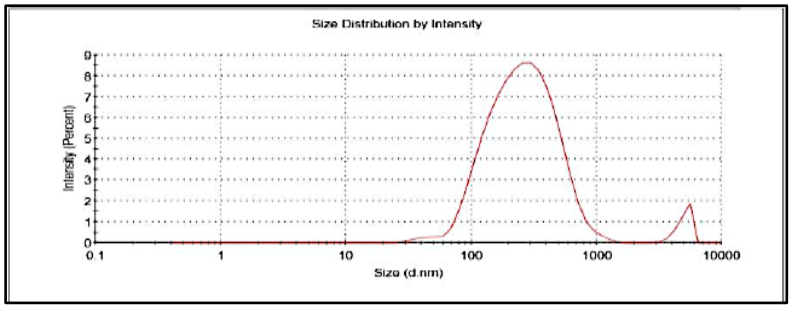


**Fig. 7a: Particle size data of optimized NS of CUR**

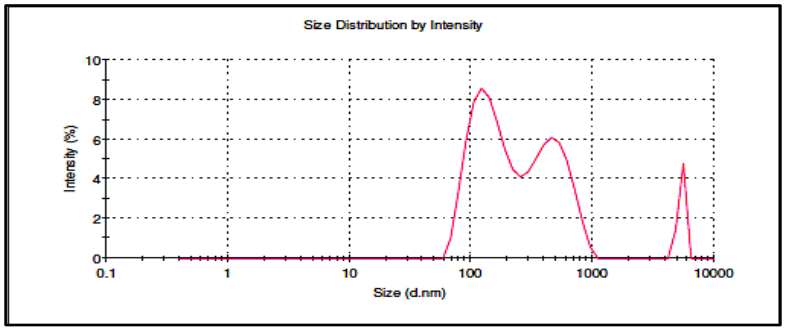


**Fig. 7b) Particle size data of redispersed NS loaded oral thin films of CUR**

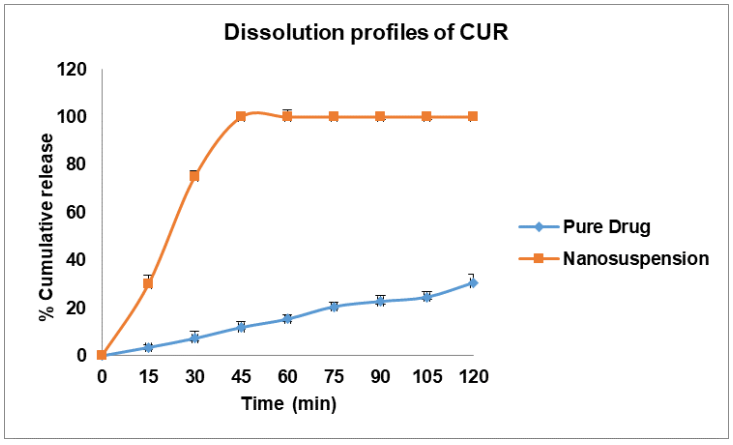


**Fig. 8a: Comparative dissolution profiles of pure drug and CUR nanosuspension**

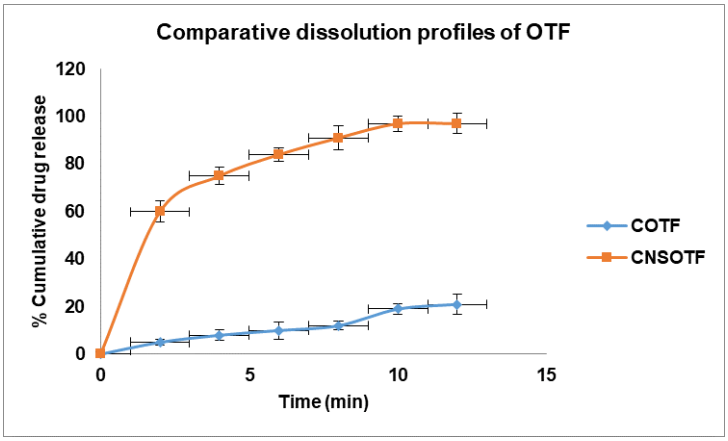


**Fig. 8b: Comparative dissolution profiles of oral thin films of pure drug (COTF) and oral thin films of nanosuspension (CNSOTF)**

**Stability of OTFs**

Accelerated stability testing (40 °C/75% RH, 3 mo) demonstrated that CNSOTF retained its mechanical integrity, dissolution profile, and nanoparticle size upon redispersion. No significant changes in appearance, drug content, or PDI were observed, confirming robust physical stability.

Various studies have been conducted in the past to enhance solubility of CUR by preparing its NS; however most of these reports anti solvent technique for preparation that requires organic solvents. In this study, atop-down approach using high-shear homogenization (HSH) was employed for NS preparation, as it is a straightforward wet-milling process where solid particles suspended in anaqueousliquid medium are subjected to intense shear forces. Unlike conventional stirring, HSH generates substantially higher shear through rotor–stator action, creating turbulence and cavitation that facilitate effective particle size reduction [24].

Kaur *et al.* formulated a curcumin nanosuspension using an antisolvent technique and optimized it with a Box–Behnken design [25]. Their optimized batch exhibited a particle size of 760 nm and a PDI of 0.445, both of which were higher than those obtained in the present study. These findings indicate that high-shear homogenization can achieve smaller particle sizes without the use of organic solvents, highlighting its potential as a greener technological approach.

The factorial design efficiently identified surfactant concentration and homogenization time as critical formulation and process parameters influencing particle size, polydispersity index (PDI), and drug loading.

In this study, a combination of sodium lauryl sulfate (SLS), an anionic surfactant providing electrostatic stabilization, and poloxamer 188, a non-ionic surfactant providing steric stabilization, as stabilizers was used. This dual stabilization strategy has been reported earlier to produce a synergistic effect, improving physical stability in nanosuspensions of poorly water-soluble drugs [26]. Inadequate amounts of stabilizer fail to fully wet the hydrophobic drug surface, while excessive amounts can lead to suboptimal size reduction [27]. Here, increasing SLS concentration led to smaller particle sizes, likely due to improved wetting and reduced interfacial tension, which facilitated particle breakage.

Likewise, prolonged homogenization time further reduced particle size by extending exposure to high shear. Both these selected parameters also lowered the polydispersity index (PDI), indicating a shift toward a more uniform particle size distribution. The observed trends suggest that optimal surfactant concentration enables homogeneous wetting, while extended homogenization ensures efficient breakage and dispersion [28].

Drug loading was also influenced by both these factors. Longer homogenization times increased drug loading by enhancing breakage kinetics and generating a higher proportion of nanosized particles. Similarly, optimal SLS concentration improved drug loading through complete surface wetting and maximal size reduction.

Furthermore, the close agreement between predicted and experimental results confirmed the robustness of the chosen optimization model.

Nanosizing significantly improved CUR's aqueous solubility-by approximately 15-fold-due to the marked increase in surface area. FTIR spectra revealed no significant chemical interactions between CUR and the excipients. DSC and XRPD revealed slight alterations in the original physical state of CUR. The optimized NS also showed a rapid dissolution profile, with nearly fivefold higher drug release compared to unprocessed CUR, consistent with the Noyes–Whitney relationship between surface area and dissolution rate [29].

Despite the substantial *in vitro* improvements, *in vivo* pharmacokinetic gains were modest. This aligns with CUR's classification as a BCS class IV drug, where permeability becomes the rate-limiting step once dissolution is no longer a bottleneck. The NS achieved ~1.2-fold higher relative bioavailability compared to the coarse suspension, with an extended Tmax. The latter may be due to the nanosized particles' prolonged suspension in gastrointestinal fluids and enhanced mucosal adhesion [30]. Therefore, future enhancement strategies may require combining nanosizing with permeability enhancers, lipid carriers, or prodrug approaches.

Scarce data is present in support of suitable solidification strategies for NS which often presents lack of commercialization prospects of NS as a final finished dosage form. Although freeze drying [31] and spray drying techniques [32] have been reported earlier for solidifying NS but they often presents long term stability challenges for hygroscopic molecules; and dosage non uniformity. Solidification of NS addresses two critical challenges: enabling a practical unit dosage form and improving long-term stability. In this study, these well-recognised challenges were addressed by successfully converting it into oral thin films (OTFs) using HPMC E15 as the hydrophilic film-forming polymer and PEG 400 as a plasticizer. HPMC E15 facilitated rapid disintegration in simulated saliva, while PEG 400 imparted mechanical strength. Both NS-loaded and pure drugfilms exhibited comparable physicochemical properties, with NS films showing higher assay values within pharmacopoeial limits, likely due to better dispersion and mixing of uniformly suspended nanoparticles.

Redispersibility studies confirmed that the nanosized particles retained their original characteristics post-solidification. The prepared OTF of NS could maintain a redispersed particle size close to the original particle size (277 nm vs 259 nm). The high viscosity of the HPMC dispersion before casting likely prevented aggregation during drying, thereby ensuring stability. The hydrophilic matrix of the OTF further enhanced dissolution velocity of the embedded nanosized CUR, combining the solubility benefits of nanonization with the convenience and stability of a solid dosage formconfirming their suitability as a final, commercially viable product.

Overall, this research highlights the dual benefits of nanosuspension technology and solid oral film formulation. The QbD approach ensured a reproducible process and an optimized product, while the solidified format addressed stability and patient compliance issues inherent to liquid nanosuspensions.

## CONCLUSION

A nanosuspension (NS) of the poorly water-soluble drug curcumin (CUR) was successfully developed using high-shear homogenization and a Quality-by-Design (QbD) approach. Formulation optimization via factorial design demonstrated that both the type and concentration of stabilizers, as well as homogenization speed and time, significantly influenced critical quality attributes. The Poloxamer 188–SLS combination provided effective electrostatic and steric stabilization, yielding a stable nanosized dispersion. Characterization by XRD and DSC confirmed that CUR retained its crystalline nature post-processing. The optimized NS exhibited markedly improved saturation solubility and dissolution rates compared with pure drug. Pharmacokinetic evaluation indicated modestly enhanced oral performance of the nanoformulation. Conversion of the liquid NS into oral thin films (OTFs) produced a stable, rapidly disintegrating, and patient compliant solid dosage form. This dual approach of nanonization coupled with solidificationoffers a scalable strategy for enhancing the delivery of poorly soluble drugs. Future work should focus on optimization of OTF formulations and *in vivo* bioavailability studies to further evaluate the therapeutic potential of NS-loaded OTFs.

## ACKNOWLEDGEMENT

The authors would like to acknowledge Zim Laboratories Limited, Kalmeshwar, India and Matrix Life Sciences, Aurangabad, India for providing gift samples for the research. The authors would also like to acknowledge VNS Faculty of Pharmacy, Bhopal, India for their support in animal studies.

## FUNDING

Nil

## AUTHORS CONTRIBUTIONS

Shobha Ubgade: Investigation, experimentation, data curation, conceptualization, and writing of original draft; Shubham Gupta: experimentation, reviewing; Vaishali Kilor and Nidhi Sapkal: conceptualization, reviewing, and supervision; Krishnakant Bhelkar: Experimentation, Alok Ubgade: Reviewing.

## CONFLICT OF INTERESTS

Declared none

## REFERENCES

1. Ipar VS, Dsouza A, Devarajan PV. Enhancing curcumin oral bioavailability through nanoformulations. Eur J Drug Metab Pharmacokinet. 2019;44(4):459-80. doi: 10.1007/s13318-019-00545-z, PMID 30771095.
2. Mohanty C, Das M, Sahoo SK. Emerging role of nanocarriers to increase the solubility and bioavailability of curcumin. Expert Opin Drug Deliv. 2012;9(11):1347-64. doi: 10.1517/17425247.2012.724676, PMID 22971222.
3. Li X, Uehara S, Sawangrat K, Morishita M, Kusamori K, Katsumi H. Improvement of intestinal absorption of curcumin by cyclodextrins and the mechanisms underlying absorption enhancement. Int J Pharm. 2018;535(1-2):340-9. doi: 10.1016/j.ijpharm.2017.11.032, PMID 29157961.
4. Ajay S, Harita D, Tarique M, Amin P. Solubility and dissolution rate enhancement of curcumin using Kollidon Va64 by solid dispersion technique. Int J PharmTech Res. 2012;4(3):1055-64.
5. Setthacheewakul S, Mahattanadul S, Phadoongsombut N, Pichayakorn W, Wiwattanapatapee R. Development and evaluation of self-microemulsifying liquid and pellet formulations of curcumin and absorption studies in rats. Eur J Pharm Biopharm. 2010;76(3):475-85. doi: 10.1016/j.ejpb.2010.07.011, PMID 20659556.
6. Ching YC, Gunathilake TM, Chuah CH, Ching KY, Singh R, Liou NS. Curcumin/Tween 20-incorporated cellulose nanoparticles with enhanced curcumin solubility for nano-drug delivery: characterization and *in vitro* evaluation. Cellulose. 2019;26(9):5467-81. doi: 10.1007/s10570-019-02445-6.
7. Gao Y, Wang C, Sun M, Wang X, Yu A, Li A. *In vivo* evaluation of curcumin loaded nanosuspensions by oral administration. J Biomed Nanotechnol. 2012;8(4):659-68. doi: 10.1166/jbn.2012.1425, PMID 22852475.
8. Ratnatilaka Na Bhuket P, El Magboub A, Haworth IS, Rojsitthisak P. Enhancement of curcumin bioavailability via the prodrug approach: challenges and prospects. Eur J Drug Metab Pharmacokinet. 2017 Jun 1;42(3):341-53. doi: 10.1007/s13318-016-0377-7, PMID 27683187.
9. Khadka P, Ro J, Kim H, Kim I, Kim JT, Kim H. Pharmaceutical particle technologies: an approach to improve drug solubility dissolution and bioavailability. Asian J Pharm Sci. 2014;9(6):304-16. doi: 10.1016/j.ajps.2014.05.005.
10. Nangare KA, PS, VK K, SR P, SA P. Therapeutics applications of nanosuspension in topical/mucosal drug delivery. J Nanomed Res Ther. 2018;7(1):1-11.
11. Wang Y, Zheng Y, Zhang L, Wang Q, Zhang D. Stability of nanosuspensions in drug delivery. J Control Release. 2013;172(3):1126-41. doi: 10.1016/j.jconrel.2013.08.006, PMID 23954372.
12. Chogale M, Gite S, Patravale V. Comparison of media milling and microfluidization methods for engineering of nanocrystals: a case study. Drug Dev Ind Pharm. 2020;46(11):1763-75. doi: 10.1080/03639045.2020.1821046, PMID 32912040.
13. Puglia C, Offerta A, Rizza L, Zingale G, Bonina F, Ronsisvalle S. Optimization of curcumin-loaded lipid nanoparticles formulated using high shear homogenization SH and ultrasonication S) methods. J NanosciNanotechnol. 2013;13(10):6888–93.
14. Kilor V, Sapkal N, Daud A, Humne S, Gupta T. Development of stable nanosuspension loaded oral films of glimepiride with improved bioavailability. Int J Appl Pharm. 2017;9(2):28-33. doi: 10.22159/ijap.2017v9i2.16714.
15. Pardeshi CV, Rajput PV, Belgamwar VS, Tekade AR, Surana SJ. Novel surface-modified solid lipid nanoparticles as intranasal carriers for ropinirole hydrochloride: application of factorial design approach. Drug Deliv. 2013;20(1):47-56. doi: 10.3109/10717544.2012.752421, PMID 23311653.
16. Shekhawat P, Pokharkar V. Risk assessment and QbD-based optimization of an Eprosartan mesylate nanosuspension: *in vitro* characterization PAMPA and *in vivo* assessment. Int J Pharm. 2019;567:118415. doi: 10.1016/j.ijpharm.2019.06.006, PMID 31175989.
17. Shegokar R, Muller RH. Nanocrystals: industrially feasible multifunctional formulation technology for poorly soluble actives. Int J Pharm. 2010;399(1-2):129-39. doi: 10.1016/j.ijpharm.2010.07.044, PMID 20674732.
18. Obeidat WM, Sallam AS. Evaluation of tadalafil nanosuspensions and their PEG solid dispersion matrices for enhancing its dissolution properties. AAPS PharmSciTech. 2014;15(2):364-74. doi: 10.1208/s12249-013-0070-y, PMID 24402462.
19. Hong J, Liu Y, Xiao Y, Yang X, Su W, Zhang M. High drug payload curcumin nanosuspensions stabilized by mPEG-DSPE and SPC: *in vitro* and *in vivo* evaluation. Drug Deliv. 2017;24(1):109-20. doi: 10.1080/10717544.2016.1233589, PMID 28155567.
20. Karki S, Kim H, Na SJ, Shin D, Jo K, Lee J. Thin films as an emerging platform for drug delivery. Asian J Pharm Sci. 2016;11(5):559-74. doi: 10.1016/j.ajps.2016.05.004.
21. Chonkar AD, Rao JV, Managuli RS, Mutalik S, Dengale S, Jain P. Development of fast dissolving oral films containing lercanidipine HCl nanoparticles in semicrystalline polymeric matrix for enhanced dissolution and ex vivo permeation. Eur J Pharm Biopharm. 2016;103:179-91. doi: 10.1016/j.ejpb.2016.04.001, PMID 27063592.
22. De SB, Shen CY, Yuan XD, Bai JX, Lv QY, Xu H. Development and characterization of an orodispersible film containing drug nanoparticles. Eur J Pharm Biopharm. 2013;85;3(B):1348-56.
23. Gulsun T, Gursoy RN, Oner L. Design and characterization of nanocrystal formulations containing ezetimibe. Chem Pharm Bull (Tokyo). 2011;59(1):41-5. doi: 10.1248/cpb.59.41, PMID 21212545.
24. Kaur J, Bawa P, Rajesh SY, Sharma P, Ghai D, Jyoti J. Formulation of curcumin nanosuspension using box-behnken design and study of impact of drying techniques on its powder

characteristics. Asian J Pharm Clin Res. 2017;10(16):43-51. doi: 10.22159/ajpcr.2017.v10s4.21335.

25. Oktay AN, Ilbasmis Tamer S, Karakucuk A, Celebi N. Screening of stabilizing agents to optimize flurbiprofen nanosuspensions using experimental design. J Drug Deliv Sci Technol. 2020;57:101690. doi: 10.1016/j.jddst.2020.101690.
26. Sun W, Mao S, Shi Y, Li LC, Fang L. Nanonization of itraconazole by high-pressure homogenization: stabilizer optimization and effect of particle size on oral absorption. J Pharm Sci. 2011;100(8):3365-73. doi: 10.1002/jps.22587, PMID 21520089.
27. Triplett MD, Rathman JF. Optimization of β-carotene-loaded solid lipid nanoparticles preparation using a high shear homogenization technique. J Nanopart Res. 2009;11(3):601-14. doi: 10.1007/s11051-008-9402-3.
28. Kocbek P, Baumgartner S, Kristl J. Preparation and evaluation of nanosuspensions for enhancing the dissolution of poorly soluble drugs. Int J Pharm. 2006;312(1-2):179-86. doi: 10.1016/j.ijpharm.2006.01.008, PMID 16469459.
29. Dhapte V, Kadam V, Pokharkar V. Pyrimethamine nanosuspension with improved bioavailability: *in vivo* pharmacokinetic studies. Drug Deliv Transl Res. 2013;3(5):416-20. doi: 10.1007/s13346-012-0112-0, PMID 25788349.
30. Stark B, Pabst G, Prassl R. Long-term stability of sterically stabilized liposomes by freezing and freeze-drying: effects of cryoprotectants on structure. Eur J Pharm Sci. 2010;41(3-4):546-55. doi: 10.1016/j.ejps.2010.08.010, PMID 20800680.
31. Hu J, Ng WK, Dong Y, Shen S, Tan RB. Continuous and scalable process for water-redispersible nanoformulation of poorly aqueous soluble APIs by antisolvent precipitation and spray-drying. Int J Pharm. 2011;404(1-2):198-204. doi: 10.1016/j.ijpharm.2010.10.055, PMID 21056643.